JOURNAL OF GEOPHYSICAL RESEARCH, VOL. 105, NO. B7, PAGES 16,279–16,294, JULY 10, 2000

A method of combining ICESat and GRACE satellite data to constrain Antarctic mass balance

John Wahr
Department of Physics and Cooperative Institute for Research in Environmental Sciences
University of Colorado, Boulder

Duncan Wingham
Department of Space and Climate Physics, University College London

Charles Bentley
Department of Geology and Geophysics, University of Wisconsin, Madison

Abstract. Measurements from the Geoscience Laser Altimeter System (GLAS) aboard NASA's ICESat satellite (2001 launch) will be used to estimate the secular change in Antarctic ice mass. We have simulated 5 years of GLAS data to infer the likely accuracy of these GLAS mass balance estimates. We conclude that ICESat will be able to determine the linear rate of change in Antarctic ice mass occurring during those 5 years to an accuracy of ~7 mm/yr equivalent water thickness when averaged over the entire ice sheet. By further including the difference between the typical 5-year trend and the long-term (i.e., century-scale) trend, we estimate that GLAS should be able to provide the long-term trend in mass to an accuracy of about ±9 mm/yr of equivalent water thickness, corresponding to an accuracy for the Antarctic contribution to the century-scale global sea level rise of about ±0.3 mm/yr. For both cases the principal error sources are inadequate knowledge of postglacial rebound and of complications caused by interannual and decadal variations in the accumulation rate. We also simulate 5 years of gravity measurements from the NASA and Deutsches Zentrum für Luft-und Raumfahrt (DLR) satellite mission Gravity Recovery and Climate Experiment (GRACE)(2001 launch). We find that by combining GLAS and GRACE measurements, it should be possible to slightly reduce the postglacial rebound error in the GLAS mass balance estimates. The improvement obtained by adding the gravity data would be substantially greater for multiple, successive altimeter and gravity missions.

1. Introduction

Climate models used to study the effects of atmospheric greenhouse gases predict an overall increase in global temperature over the next century of between 1°and 3.5°C [*Houghton et al.*, 1996]. An increase of this magnitude could have numerous catastrophic effects, not the least of which might be a significant global rise in sea level caused by a combination of melting ice sheets and thermal expansion of sea water.

The global rate of sea level rise during the last century has apparently been between 1 and 2.5 mm/yr (for a review, see *Houghton et al.* [1996]). The mechanisms responsible for this sea level rise are not entirely understood. Changes in Antarctic ice are a potentially important source of sea level variability but are not well known. *Houghton et al.* [1996] conclude that the contribution of the Antarctic ice sheet to global sea level rise averaged over the past century could be anywhere from -1.4 to +1.4 mm/yr.

A good estimate of the present-day contribution of Antarctica to sea level change would increase the credibility of any prediction of how the Antarctic ice sheet might behave in the future. An important step toward estimating present-day Antarctic and Greenland mass balance will be the 2001 launch of NASA's Ice, Cloud, and Land Elevation Satellite (ICESat), which will carry the Geoscience Laser Altimeter System (GLAS) laser altimeter, and will have a mission lifetime of 3-5 years. To study the polar ice sheets, a laser pulse generated by the altimeter will reflect off the snow/ice surface and return to the satellite. The round-trip distance will be measured and combined with on board Global Position-

Paper number 2000JB900113.
0148-0227/00/2000JB900113$09.00

ing System (GPS) measurements of the geocentric position of the spacecraft to map out changes in the surface elevation of the polar ice sheets at regular time intervals. The exact repeat period of the ground tracks will be 183 days, though there will be a 25-day near-repeat subcycle. Changes in the ice sheet elevation will be determined from crossover differences.

Using GLAS data, it will be possible to estimate the secular change in total Antarctic mass over the mission lifetime. Five years of radar altimetry from ERS-1, covering 63% of the grounded ice sheet and concentrated away from the margins, have shown no sign of the large imbalances considered as upper bounds by *Houghton et al.* [1996] [*Wingham et al.*, 1998]. With ICESat it will be possible to also consider the marginal regions of the ice sheet and to extend the coverage closer to the pole.

The GLAS estimate of the 5-year trend in mass balance will be subject to a variety of errors. In addition, the 5-year trend will not necessarily equal the century-scale trend. We address these issues in this paper and determine the accuracy with which GLAS will be able to determine both the 5-year and multicentury trends.

The largest error sources for determining the trend in mass are uncertainties in postglacial rebound (PGR) and complications caused by decadal and interannual variability in accumulation rate. PGR causes vertical uplift of the crust underneath Antarctica, and this maps directly into an apparent change in ice thickness. We show that the PGR signal can be reduced by combining the GLAS altimeter data with gravity measurements from the Gravity Recovery and Climate Experiment (GRACE) dedicated-gravity satellite mission. GRACE is under the joint sponsorship of NASA and the Deutsches Zentrum für Luft-und Raumfahrt. Scheduled for a 2001 launch with a nominal 5-year lifetime, GRACE consists of two satellites in low-Earth orbit (an initial altitude in the range of 450-500 km) and a few hundred kilometers apart that range to each other using microwave phase measurements. Onboard GPS receivers will determine the position of each spacecraft in a geocentric reference frame. Onboard accelerometers will be used to detect the nongravitational acceleration so that its effects can be removed from the satellite-to-satellite distance measurements. The residuals will be used to map the gravity field. The gravity field will be determined orders of magnitude more accurately, and to considerably higher resolution, by GRACE than by any existing satellite. This will permit temporal variations in gravity to be determined down to scales of a few hundred kilometers and shorter every few weeks. These temporal variations can be used to study a large number of problems in a number of disciplines, from monitoring changes in water, snow, and ice on land, to determining changes in seafloor pressure, to studying PGR within the solid Earth. Comprehensive descriptions of these and other applications are given by *Dickey et al.* [1997] and *Wahr et al.* [1998].

In this paper, we describe a method of combining GLAS and GRACE data to estimate the secular change in ice mass averaged over Antarctica. We assess the uncertainty with which this mass balance can be determined, both by using GLAS alone and by combining with GRACE. We do this by constructing 5 years of simulated GLAS and GRACE data, including contributions from a realization of the expected GLAS and GRACE measurement errors and from a comprehensive set of expected geophysical signals. We use these data to infer the Antarctic mass balance and then compare with the value used to construct the simulation. The difference is equal to the error in the satellite mass balance estimate. We do this for a large number of 5-year simulated periods, so as to be able to characterize the error more fully.

Throughout this paper, we will describe changes in mass in terms of mm/yr of equivalent water thickness. Note that a change in thickness of 1 mm/yr of water is equivalent to a change in surface mass density of 1 $(\mathrm{kg/m^2})/\mathrm{yr}$; or, assuming an ice density of 917 $(\mathrm{kg/m^3})$, to 1.09 mm/yr of ice thickness.

2. Constructing Simulated Data

In this section we describe our method of simulating the GLAS and GRACE data. For each satellite we construct the data as the sum of geophysical signals and satellite measurement errors.

For GRACE we simulate 5 years of monthly measurements of the geoid. It is usual to expand the geoid as [see, e.g., *Wahr et al.*, 1998]

$$N(\theta,\phi) = a\sum_{l=0}^{\infty}\sum_{m=0}^{l}\tilde{P}_{lm}(\cos\theta)[C_{lm}\cos(m\phi) + S_{lm}\sin(m\phi)], \quad (1)$$

where θ and ϕ are colatitude and eastward longitude, the $\tilde{P}_{lm}$ are normalized associated Legendre functions, a is the Earth's radius, and the C_{lm} and S_{lm} are dimensionless geoid coefficients that GRACE will deliver every few weeks. For our simulations we construct 5 years of monthly C_{lm} and S_{lm}, up to a maximum degree and order (i.e., l and m) of 100.

For GLAS we simulate 5 years of monthly ice sheet elevations, sampled on a grid with uniform 2.25° spacing in latitude and 3.75° spacing in longitude. It is unlikely that the actual GLAS measurements of crossover differences will be combined into gridded values with exactly this spatial and temporal resolution. A temporal resolution of 6 months or longer is more probable, given that 6 months is the exact repeat period of the satellite (though the satellite orbit will have a 25-day near-repeat subcycle, which could conceivably permit monthly resolution, if desired). Furthermore, the GLAS crossover differences will be used to find changes in elevations, rather than to find the elevations themselves.

Our decision to simulate elevation fields instead of changes in elevations, and to assume monthly values instead of values every 6 months or longer, was made simply for convenience. It was based partly on the fact that the precipitation fields used to construct the simulated data (see below) are given at monthly intervals. Our spatial resolution was chosen arbitrarily. In section 2.3 below, we will choose our GLAS measurement errors in such a way that the uncertainty in the secular trend determined from our simulated data agrees with the uncertainty that would be obtained directly from the crossovers.

We assume that the GLAS data are available all the way to the pole. In reality the orbit will have a 94° inclination, so there will be no data within 4° $\approx$ 450 km of the pole (though GLAS will have the capability of off-nadir pointing, which could increase the coverage by up to 1 additional degree closer to the pole). However, since this missing region comprises only 5% of the ice sheet and is arid in any case, including simulated data from this region should have only a small effect on our conclusions and simplifies the inversion process considerably.

For GLAS our simulated monthly ice sheet elevations consist of contributions from snow accumulation and uniform horizontal ice flow on Antarctica, of PGR in the solid Earth, and of GLAS measurement errors. For GRACE our simulated monthly C_{lm} and S_{lm} include the effects of snow accumulation and uniform ice flow on Antarctica, of PGR, of redistribution of mass in the ocean and in the storage of water and snow over all continental regions outside of Antarctica, of errors in atmospheric pressure, and of GRACE measurement errors.

2.1. Snow and Ice Simulation

To estimate the contributions of Antarctic snow accumulation for both GLAS and GRACE, we use monthly precipitation values output from the National Center for Atmospheric Research (NCAR) Climate System Model (CSM-1), [G. Bonan, personal communication, 1997] computed on a 2.9° by 2.9° grid [see, e.g., *Boville and Gent*, 1998]. This model couples together component models of the atmosphere, ocean, sea ice, and land surface processes. After an initial spin-up procedure, in which the individual component models are run separately, the models are coupled together into a 300-year integration. In our analysis we use precipitation fields from years 81-299 of the coupled model integration. Years 1-80 are not included because there is some evidence that the fields in those years may include a residual drift due to incomplete spin-up of the model. This model run is not meant to represent any particular 300-year time span. Rather, our assumption is only that the amplitudes and the spatial and temporal characteristics of Antarctic precipitation are reasonably well represented by the model output.

This is a hard assumption to assess, because of lack of data to compare with. The atmospheric component model used in CSM-1 is the latest version of the NCAR Community Climate Model, CCM3. This model can be run in a stand-alone mode, by specifying monthly mean sea surface temperature values and sea ice distributions as ocean boundary conditions. *Briegleb and Bromwich* [1998] compare the output from CCM3 run in this fashion for 1979-1993 with the annual mean precipitation fields generated by the European Centre for Medium-Range Weather Forecasts (ECMWF) for the same time period. They find that the annual mean Antarctic precipitation predicted by CCM3 tends to be somewhat smoother than that predicted by the ECMWF. However, the amplitudes and general spatial patterns of the CCM3 annual mean tend to agree well with those from the ECMWF. They find annual polar cap (70°-90°S) means for precipitation minus evaporation and sublimation that are 18.1 cm/yr for CCM3, 14.6 cm/yr for ECMWF, and 18.4 $\pm$ 3.7 cm/yr for the ground-based observational estimates of *Giovinetto et al.* [1992]. We know of no attempt to assess the time-variable components of the CSM-1 Antarctic precipitation fields.

The precipitation fields describe the rate at which water from the atmosphere is deposited on the Earth's surface. For the real Antarctic ice sheet the horizontal flow of ice redistributes the water mass and eventually releases it to the ocean. This ice flow, which is not included within the CSM-1 model, is likely to be constant over long timescales in most places [see, e.g., *Oerlemans*, 1981], although searching for evidence of nonconstant flow is one of the primary objectives of the ICESat mission.

To simulate the mass balance of Antarctica for inclusion into our synthetic satellite data, we proceed as follows. First, we find the 219-year mean of the CSM-1 precipitation fields at every grid point and remove those mean gridded values from each monthly precipitation field. We remove the mean values because they are very large but irrelevant: They will presumably be nearly balanced by the steady horizontal flow of ice. Second, we integrate the resulting residual precipitation fields over time. This results in a 219-year time series for the accumulated mass at every grid point caused by the variable part of the accumulation rate. These accumulation fields have no century-scale trend, since we removed the mean of the precipitation fields before integrating. When we refer to the accumulation fields in the remainder of this paper, we mean these residual, detrended fields.

Third, we subtract an additional 30 mm/yr of equivalent water thickness at every grid point, so that the long-term mass trend at each grid point is a net loss of 30 mm/yr of water thickness. This 30 mm/yr is a purely ad hoc value for the century-scale trend, inserted only to provide a nonzero trend for the simulations. It could, though, just as well have been chosen to be 0

mm/yr or to have been spatially variable. It represents the combined effects of the long-term horizontal ice flow and the average accumulation over 219 years. Because the method we will use to infer mass balance is linear, our final conclusions about the accuracy of the GLAS and GLAS plus GRACE estimates would be the same if we had not subtracted this additional 30 mm/yr. Note that the secular mass variability averaged over 5 years will likely differ from a uniform 30-mm/yr mass loss, because the secular change in accumulated mass over 5 years will differ from the secular change over 219 years.

We combine these surface mass estimates of the variable accumulation and the long-term mean and integrate over latitude and longitude to find a time series for the geoid coefficients C_{lm} and S_{lm} [see *Wahr et al.*, 1998, equations (11) and (12)]. We include the elastic response of the solid Earth in our estimated geoid coefficients (represented by the load Love number k_l in equation (12) of *Wahr et al.*). These geoid coefficients are included in our simulated GRACE data.

Estimating the contributions to GLAS ice elevation measurements is more complicated. To simulate the change in elevation from our variable mass fields, it is necessary to assume something about the density of snow and ice. The density of newly fallen snow is assumed here to be $\rho_s = 300$ kg/m^3. Snow compacts with age and as more snow falls on top of it, eventually reaching the density of the underlying ice, which we assume is $\rho_i = 917$ kg/m^3. The transition from ρ_s to ρ_i depends both on the compressibility of the snow and on the rate at which more snow is added to the top of the column: i.e., on the accumulation rate.

Suppose that the accumulation rate is constant over long times. Then the vertical density profile at the top of the ice column will eventually reach a steady state situation, so that for every 1 mm of water that gets added to the top of the column in the form of snow, an equivalent 1 mm of water finishes getting compressed to the density of ice at the ice-snow interface. Thus in the limit of constant accumulation rate, and ignoring the possibility of horizontal flow out of the snow-ice column, the rate of increase in surface elevation will equal the rate of increase in mass, divided by ρ_i. This is the relation we use to convert the long-term 30-mm/yr secular change in equivalent water mass (caused by a combination of ice flow and century-scale accumulation) to a secular elevation change.

At the other extreme, suppose that there are variations in accumulation with periods extremely short compared to the compaction time of the snow. The column will then not have sufficient time to compact in response to the variation in overlying pressure, and so the change in surface elevation will equal the change in accumulating mass, divided by ρ_s.

These are limiting cases of a more general relation between the variable accumulation rate $\dot{m}_s(t)$ and the rate of change in ice sheet thickness $\dot{h}_i(t)$ caused by that variable accumulation. Let $\dot{\mathbf{h}}_\mathbf{i}(\omega)$ be the Fourier transform of $\dot{h}_i(t)$ at angular frequency ω, and let $\dot{\mathbf{m}}_\mathbf{s}(\omega)$ be the Fourier transfrom of $\dot{m}_s$. Then *Wingham* [2000, equation 33] describes the relation between these quantities as

$$\dot{\mathbf{h}}_\mathbf{i}(\omega) = H_m(\omega)\,\dot{\mathbf{m}}_\mathbf{s}(\omega) \tag{2}$$

where $H_m(\omega)$ is the transfer function representing the compaction of snow into ice. (Here we have ignored the $H_\rho\,\dot{\rho}_s$ term in Wingham's equation (33) which accounts for the contribution of temporal variations in the density of newly fallen snow. As argued by Wingham, field observations of near-surface density show such short-scale variability that it is reasonable to assume that the term is negligible in areal averages of the size considered here.) When we use (2) to estimate changes in thickness, will use values for $H_m(\omega)$ determined using the model of *Arthern and Wingham* [1998], with their values of compaction conditions at Byrd, West Antarctica. These are close to average conditions for the grounded Antarctic ice sheet. The limiting cases are $H_m(\omega) \to 1/\rho_i$ as $\omega \to 0$ and $H_m(\omega) \to 1/\rho_s$ as $\omega \to \infty$.

To generate a synthetic time series of ice sheet elevations, we find the Fourier transform of the first 2048 months (= 170.67 years; 2048 is a power of 2, which makes it possible to use fast Fourier transform algorithms) of CSM-1 Antarctic precipitation fields at every grid point, after first removing the 219-year mean from the precipitation fields (see above). We use those results in (2) to find the Fourier transform of the surface elevation, take the inverse Fourier transform to infer the rate of change in ice sheet elevation in the time domain, and then integrate over time to get the ice sheet elevation at every grid point for each of the 2048 months. We add these elevations to the contributions from the -30 mm/yr long-term trend, computed assuming a uniform density of $\rho = \rho_i$, as described above.

We estimate the elastic vertical displacement U of the solid Earth caused by the mass load, using standard methods (see, e.g., equations (40) and (42) of *Mitrovica et al.* [1994], setting $W_{lm} = 0$ in those equations). We use elastic load Love numbers, h_l (denoted as $h_l^{L.E}$ by Mitrovica et al.), computed for the preliminary reference Earth model PREM [*Dziewonski and Anderson*, 1981] and provided by D. Han (personal communication, 1995). We add U to our simulated ice sheet elevations and include the total elevation results in the synthetic GLAS data at each grid point.

2.2. Simulation of Postglacial Rebound

Because the solid Earth is a viscoelastic body, it is still adjusting to the accumulation and subsequent melting of ice that occurred during and after the last ice age. Included in this adjustment are secular uplift of the crust underlying Antarctica in response to the Holocene reduction of the Antarctic ice load and a corresponding

secular increase in the gravitational field over Antarctica as material in the mantle flows in horizontally from surrounding regions (for a recent description of these possible signals over Antarctica, see *James and Ivins* [1998]. Consequently, there will be PGR contributions both to ice sheet elevations as measured by GLAS and to the gravity field as measured by GRACE. For GLAS for example, uplift of the crust will cause uplift of the entire overlying ice column, and so the ice surface elevations would increase even if there were no change in ice mass. The Earth is also still adjusting viscoelastically to whatever changes might have occurred in Antarctic ice since the last ice age, and this causes additional crustal motion (which could be either uplift or subsidence, depending on the details of the ice mass history and the mantle's viscosity profile). We refer to the Earth's viscoelastic response to the sum of all past changes in ice as the PGR signal.

If these rebound effects are not removed from the data, they will contaminate the ice mass estimates obtained from both GLAS and GRACE. The total PGR signal for Antarctica depends on the time history and spatial distribution of the Antarctic ice sheet over the last many hundred to many thousand years and on the Earth's viscosity profile. Neither of these is well known. In fact, even the uncertainties in these quantities are poorly known, which makes it difficult to assess the errors in the GLAS and GRACE ice mass solutions caused by errors in the rebound models.

To construct the synthetic GLAS and GRACE data used in this paper, we estimate the effects of PGR by convolving viscoelastic load Love numbers, computed as described by *Han and Wahr* [1995], with estimates of the Antarctic deglaciation history. We use the ICE-3G Pleistocene ice model of *Tushingham and Peltier* [1991], with the addition of a preceding 90-kyr glaciation phase to build the ice sheet. The ICE-3G deglaciation period ends 4000 years ago. To include the possibility of more recent changes in ice, we also sometimes assume an additional secular change of Antarctic ice during the last 4000 years, uniformly distributed over the ice sheet. The rate of that increase or decrease in ice is variable and is chosen to have different values for different simulation runs. Similarly, the mantle viscosity profile used to construct the viscoelastic Green's functions is varied for different simulation runs. For each run we compute the viscoelastic uplift of the crust and add it to the synthetic GLAS ice elevation data, and we compute the viscoelastic, secular contributions to the gravitational potential and add those to the synthetic GRACE data.

2.3. Satellite Measurement Errors

We include estimates of satellite measurement errors in the synthetic data for both GLAS and GRACE. For GRACE we use preliminary accuracy estimates for the geoid coefficients provided by B. Thomas and M. Watkins at the Jet Propulsion Laboratory and S. Bettadpur at the University of Texas (personal communication, 1997). These errors are described in slightly more detail by *Wahr et al.* [1998]. We include them in our synthetic monthly geoid coefficients by generating Gaussian random numbers with variances consistent with the error estimates. We assume that the errors are uncorrelated from one month to the next.

To estimate GLAS measurement errors, we use an indirect approach. *Choe* [1997] constructed simulated GLAS crossover values, including the effects of instrument noise, orbit error, pointing error, a truth model for ice surface variation, and an assumed 50% data decimation due to thick cloud cover. He concluded that by using 6 months of crossover differences, the linearly varying change in surface elevation could be determined to an accuracy of 80 mm/yr when averaged over 100 × 100-km^2 regions centered at 72°S latitude (B. Schutz, personal communication, 1999). The error averaged over any region tends to vary inversely with the square root of the number of crossover points in that region. Thus the error decreases rapidly closer to the pole, where there are many more crossover points. Also, at any given latitude the error tends to decrease inversely with the square root of the area.

For our simulation we have chosen to construct monthly, gridded elevation fields over regions of varying area (see section 2). To obtain our estimates of the secular mass balance, we will fit a mean and a trend to those simulated data. Thus we choose the value of the rms, σ, of our monthly elevation measurement errors to be such that if a mean and a trend were fit to six consecutive monthly values, the error in the trend would be 80 mm/yr when averaged over any 100 × 100-km^2 region. To be conservative, we use the 80-mm/yr value at all latitudes, even those close to the pole. To determine σ, we note that if we fit a mean and a trend to N monthly points, then the 1-sigma rms error on the trend will be $12\,\sigma\,\sqrt{12/\left[(N-1)N(N+1)\right]}$ mm/yr (the factor inside the square root comes from the covariance matrix of the fit; see, e.g., section 15.6 of *Press et al.* [1992]). By equating this to 80 mm/yr when $N = 6$, we conclude that the uncertainty in our monthly 100 × 100-km^2 averages needs to be ~ 30 mm. For every one of our 2.25° × 3.75° simulated grid elements, we scale this 30-mm monthly uncertainty estimate by $\sqrt{100 \times 100\,\mathrm{km}^2/G}$ where G is the grid element area. We include these errors in our synthetic elevation data, by generating Gaussian random numbers with the specified variance. We assume that there is no correlation between errors from one month to the next, or from one grid element to another.

We also include an additional secular GLAS error of amplitude 0.1 mm/yr (C. K. Shum, personal communication, 1998), which we add to the surface elevation at every grid point. This error is meant to represent the possible secular effects of orbit errors during the 5-year mission.

We can estimate the likely effects of these assumed satellite errors on the inferred Antarctic mass balance, prior to doing any simulations. If the snow/ice density is assumed to be 917 kg/m^3 when inferring mass balance from GLAS surface elevations, then the secular error of -0.1 mm/yr maps directly into a mass balance error of 0.0917 mm/yr of equivalent water thickness.

For the random error component the 30-mm rms error for each 100 x 100-km^2 area would lead to monthly values of the surface mass over the entire ice sheet (area approximately equal to 12 $\times 10^6$ km^2) accurate to $\sim 30\times\ 0.917\ \times\sqrt{100^2/12\times 10^6} \approx 0.8$ mm of equivalent water thickness. If we use N of these monthly GLAS estimates to fit a constant offset and secular trend, the 1-sigma error in the secular trend would be $0.8\times 12\times\sqrt{12/(N-1)N(N+1)}$ mm/yr. So for 5 years of data (N=60) the error in the trend would be on the order of 0.07 mm/yr equivalent water thickness, which is far smaller than the errors due to other sources (see sections 3 and 4). This approximate result for the effects of the satellite errors is consistent with the results of the simulation we will describe in section 5.2, in cases where we include only satellite errors in the simulated data.

2.4. Other Contributions to GRACE

The GRACE gravity measurements will also include contributions from variable mass in the ocean, the atmosphere, and the storage of water and snow over continental regions outside of Antarctica.

We include the effects of the ocean by using output from a variant of the Parallel Ocean Program ocean general circulation model developed at Los Alamos National Laboratory [*Dukowicz and Smith*, 1994], forced with both winds and pressure. The model output is used to construct monthly geoid coefficients (M. Molenaar and F. Bryan, personal communication, 1998), as described by *Wahr et al.* [1998], which are then added to the synthetic GRACE data. The inverted barometer response to pressure variability is removed from the oceanic solution prior to constructing the geoid coefficients. This removal is equivalent to adding, to the full oceanic solution, the time-variable mass signal from the atmosphere above the oceans.

We include the effects of continental water storage by using output (C. Milly and K. Dunne, personal communication, 1999) from a land-surface water and energy balance model coupled to a high-resolution climate model at the Geophysical Fluid Dynamics Laboratory in Princeton. The model generates daily, gridded estimates of soil water, snowpack, surface water, and groundwater. These are used to construct monthly averaged geoid coefficients, which are then included as part of the synthetic GRACE data. The model's predictions of water (i.e., snow) storage on Antarctica are not included, since we are using output from the NCAR climate model for that.

Variations in the distribution of atmospheric mass contribute to the time-variable geoid measured by GRACE. This variability can be modeled using global, gridded pressure fields, such as those routinely produced by such weather forecast centers as the ECMWF and the National Centers for Environmental Prediction (NCEP). We expect that the atmospheric contributions estimated from these pressure fields over land will be routinely removed from the GRACE observations, before using those observations to study Antarctic mass balance. We expect that no pressure corrections will be made over the ocean.

The pressure fields over land are not perfect, and errors in those fields could degrade the Antarctic results. To model this degradation, we estimate the errors in the monthly averaged pressure fields over land as $\delta P = (P_{\rm ECMWF} - P_{\rm NCEP})/\sqrt{2}$, where $P_{\rm ECMWF}$ and $P_{\rm NCEP}$ are the monthly averaged surface pressure fields predicted by the ECMWF and NCEP, respectively. We use δP to estimate monthly geoid coefficients and include those coefficients in our synthetic GRACE data.

We find from the simulation described in section 5.2, that none of these contributions to GRACE (i.e., from the ocean, from continental water storage outside of Antarctica, or from atmospheric pressure errors) have significant impact on our uncertainty of the secular Antarctic mass balance. This is presumably because these contributions either originate from regions far removed from Antarctica or have only a small secular component, or both. The effects of the GLAS and GRACE measurement errors are more important but are still considerably smaller than the effects of PGR and of a variable accumulation rate on GLAS, and of PGR on GRACE.

3. Error Caused by Variations in Accumulation Rate

Because of the long time constants associated with ice flow the focus of Antarctic mass balance studies is usually on mass variability at timescales of a century or longer ICESat and GRACE will have lifetimes of the order of 5 years. Suppose that the annually averaged accumulation rate were constant over timescales of centuries. Then the linear trend in mass during the 5 years of the GRACE mission would equal the century-scale mass trend. Similarly, the trend in ice sheet thickness during the 5-year ICESat mission would equal the century-scale trend in thickness. Also, for a constant accumulation rate the secular GLAS thickness estimate could be used to obtain the century-scale trend in mass by multiplying the thickness by ρ_i (see the discussion preceding equation (2)).

In reality, though, there are interannual and interdecadal variations in accumulation rate, and these cause the secular mass trend determined from 5 years of data to differ from the true multicentury trend (this issue

was first discussed by *Van der Veen* [1993]). Part of this difference occurs simply because the rate of mass change over 5 years is apt to differ from the rate of mass change over a century. For GRACE, which is directly sensitive to mass variability, this is the only issue. For GLAS, which is sensitive to ice sheet thickness rather than to mass, there is the additional problem that the relation between thickness and mass is no longer simple multiplication by ρ_i but is complicated by the variable accumulation rate. In section 2.1 we described how we include the effects of this complication in our simulated data using (2). However, (2) will probably not be useful for converting GLAS thickness measurements into mass balance estimates, because its use requires knowledge of the variable accumulation at interannual and interdecadal periods. It is unlikely that this variability will be known accurately (although GLAS measurements will help to constrain it). Instead, we expect that people will choose to convert the GLAS secular thickness estimates into secular mass estimates by multiplying by ρ_i, since this is the density appropriate for the century-scale variability. This will introduce an additional error into the GLAS mass balance estimates that does not affect GRACE.

In this section, we use our simulated satellite data to understand the likely impact a variable accumulation rate might have on the inferred century-scale trend. We will separate the effects, somewhat artificially, into the two error types described in the preceding paragraph. We will refer to the fact that a 5-year mass trend might differ from the century-scale mass trend as the "undersampling error." We will refer to the error in the GLAS mass balance estimate caused by approximating $H_m(\omega)$ in (2) with $1/\rho_i$ as the "compaction error." Note that the compaction error causes an error in the GLAS estimate of the 5-year trend (and hence also of the multicentury trend).

We can estimate the relative importance of these two error sources prior to doing any simulations. *Wingham* [2000] showed that if the variable accumulation rate at an Antarctic location is characterized by a white spectrum, then after transforming back to the time domain and integrating over a 5-year time interval, (2) is approximately equivalent to

$$h_i = \frac{m_s}{\rho_s} = \frac{m_s}{\rho_i} + \left(\frac{1}{\rho_s} - \frac{1}{\rho_i}\right) m_s\,, \qquad (3)$$

where h_i and m_s are the change in ice thickness and accumulation, respectively, over that 5-year period due to the variable accumulation rate. The m_s/ρ_i term on the right-hand side of (3) is the undersampling error while the $((1/\rho_s)$ - $(1/\rho_i))$ m_s term is the compaction error under this assumption of a white spectrum. Since $((1/\rho_s)$ - $(1/\rho_i))$ $\approx 2/\rho_i$, then the compaction error in this case is about twice the undersampling error and is in phase with it. Thus the total error caused by the variable accumulation rate in determining the century-scale trend from GLAS data is approximately 3 times the undersampling error alone and so is approximately 3 times the corresponding error in the GRACE data under this assumption of a white spectrum.

In sections 3.1 and 3.2 below, we use our simulated data to estimate absolute amplitudes for these errors and to obtain an estimate of the relative importance of the two error sources without assuming a white accumulation rate spectrum. One of our conclusions is that the ratio of the compaction error to the undersampling error is actually closer to 1.5 than to 2.

3.1. Undersampling Error

In this section we address the issue of how a secular trend in Antarctic ice mass over a 5-year period might differ from the true multicentury trend. Variations in ice mass are caused by the combined effects of accumulation and of horizontal ice flow off the continent and into the ocean. The ice flow contributions are apt to be constant over timescales of centuries. So this problem reduces to estimating how the accumulation rate averaged over 5 years is likely to differ from the accumulation rate averaged over centuries. This difference is the "undersampling error."

To construct this estimate, we use the precipitation fields output from the CSM-1 climate model, remove the mean (see section 2.1), and compute their contributions to the total Antarctic mass every month for 219 years. The residuals, which have a secular trend of zero, are shown in Figure 1a in units of equivalent water thickness. We assume that GLAS and GRACE will sample this mass and determine a secular trend over some 5-year time span. At issue is whether 5-year trends of the Figure 1a results are apt to differ substantially from zero.

We extract a series of 5-year data spans from Figure 1a and determine the trend for each of these spans. The first span begins in month 1 of year 1, the second in month 2 of year 1, etc.; the last span (the 2568th) begins in month 1 of year 215. Figure 1b shows the secular trend for each span, plotted as a function of the time of the beginning of the span. Though there are trends as large as 12 mm/yr, the rms of the trends is 3 mm/yr. Thus we tentatively conclude that a 5-year secular trend in snow-ice mass is apt to differ from the multicentury trend by roughly ±3 mm/yr of equivalent water thickness. A mass trend of 3 mm/yr corresponds to a global sea level change of ~0.1 mm/yr.

3.2. Compaction Error

The compaction error, which affects mass balance estimates from GLAS but not from GRACE, occurs because the density profile in the upper layers of the snow-ice column depends on the (unknown) variability in accumulation rate. To estimate this error, we use the CSM-1 precipitation fields (after removing the 219-year mean) and (2) to simulate 2048 months of sur-

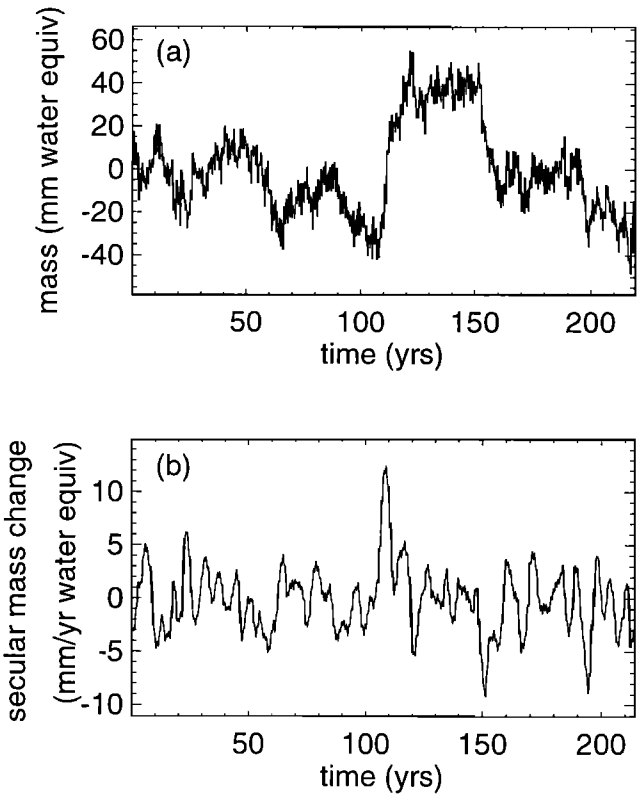

Figure 1. (a) Two hundred-nineteen years of monthly values of the snow-ice mass averaged over the Antarctic ice sheet, as predicted by the CSM-1 climate model. A mean and trend have been fit and removed. The units are equivalent water thickness. (b) Values of the secular trend in mass inferred over many 5-year intervals of the data shown in Figure 1a. The time on the x axis denotes the beginning of the 5-year interval. The values plotted in Figure 1b represent the difference between the 5-year trend and the 219-year trend that had been removed from the original data prior to these 5-year fits.

face elevations at every grid point (see section 2.1). We average the accumulation and elevation fields over the entire Antarctic continent to obtain time series for the spatially averaged mass balance and surface elevation. We extract a series of 5-year data spans from each of the two time series, as described in section 3.1, and fit a secular trend to each 5-year span. Figure 2a shows the series of 5-year-average surface mass balance rates (these are identical to the first 2048 months of values shown in the Figure 1b results and represent the undersampling error). Figure 2b shows the series of 5-year trends in average surface elevation, converted to a mass estimate by multiplying by a density of $\rho_i = 917$ kg/m^3, which is equivalent to the assumption (in this case mistaken) that the changes in elevation are related entirely to a combination of solid ice flow and of accumulation that is constant over very long (e.g., century) timescales. These Figure 2b results represent the sum of the undersampling and compaction errors.

Figure 2c is the difference between Figures 2a and 2b. We interpret the results in Figure 2c as the likely errors in 5-year secular mass estimates from GLAS, caused by not knowing the density profile. Figure 2c shows that some 5-year trends could be as large as 18 mm/yr (water thickness equivalent) but that the rms is 4.5 mm/yr. We thus conclude that the compaction error in GLAS mass balance estimates is likely to be ±4.5 mm/yr, which is equivalent to an error of about ±0.15 mm/yr in global sea level rise. Note that the compaction error is about a factor of 1.5 larger than the undersampling error, rather than the factor of 2 derived above under the assumption of a white accumulation rate spectrum.

As expected, the compaction error (Figure 2c) is reasonably well in phase with the undersampling error (Figures 1b and 2a). The sum of these two errors (Figure 2b) has an rms of 7.5 mm/yr, which is about equal to the sum of the rms values for the undersampling error (3.1 mm/yr) and the compaction error (4.5 mm/yr). This 7.5 mm/yr can be interpreted as the rms of the total error in the century-scale trend estimate caused by the variable accumulation rate.

4. Postglacial Rebound Error

To estimate the possible effects of PGR on the GLAS and GRACE mass balance estimates, we use the rebound model described in section 2.2 to estimate the contribution of the rebound to secular changes both in the ice sheet elevation and in the global gravity field. We construct a variety of estimates, using different assumptions about the Earth's viscosity profile and the ice sheet time history.

In all our Earth models we fix the lithospheric thickness at 120 km and assume the viscosity of the upper mantle (the region of the Earth between the base of the lithosphere and the seismic discontinuity at 670-km depth) to be 1.0×10^{21} Pa sec. The Earth's core is assumed to be inviscid. We consider three possible values for the viscosity of the lower mantle (the region in the mantle below 670-km depth): 4.5×10^{21} Pa sec, 1.0×10^{22} Pa sec, and 5.0×10^{22} Pa sec.

For the ice model we adopt the ICE-3G [*Tushingham and Peltier*, 1991] model for late Pleistocene deglaciation, augmented by a 90,000-year glaciation phase that ramps up the ice sheets from zero to the initial ICE-3G values. We include not only the Antarctic ice sheet but all the other ICE-3G ice sheets as well (e.g., Laurentia, Fennoscandia, Greenland). We will refer to this ice model as model A. Not surprisingly, the deformation caused by the Antarctic ice sheet has the largest effect on our results.

In ICE-3G the Antarctic ice is modeled as having begun melting 9000 years B.P., to have finished melting 4000 years B.P., and to have melted enough ice to have caused a 26-m rise in global sea level. We also consider a variant of this Antarctic component of ICE-3G, in which we represent the deglaciation using exactly the ICE-3G spatial pattern and time variability, except that we assume that all the melting occurred between 12,000 and

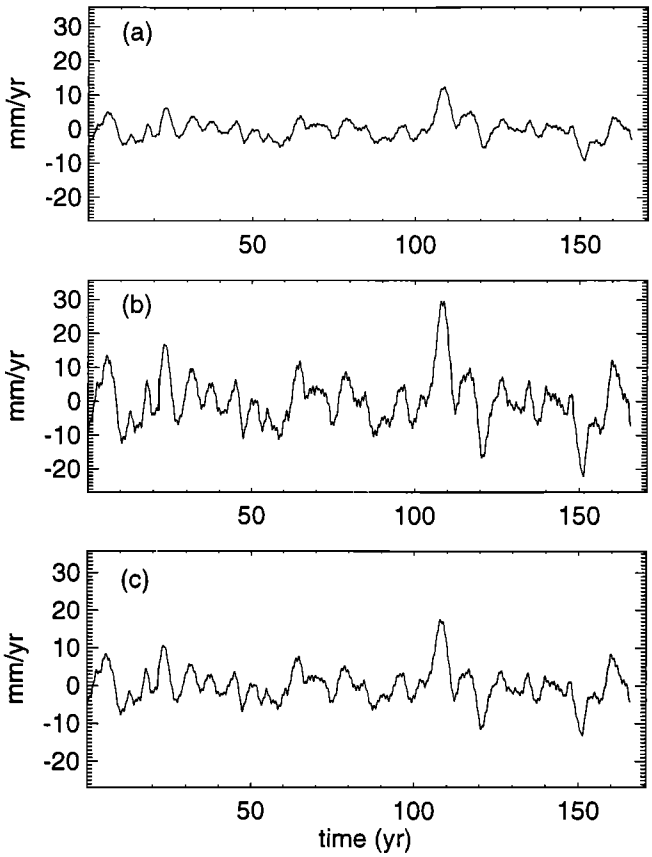

Figure 2. (a) Values of the secular trend in surface mass balance (expressed in millimeters of water per year) inferred from moving 5-year windows of the detrended data shown in Figure 1a. These are the first 2048 months of data plotted in Figure 1b, but with a different scale. (b) Five-year secular trends in surface mass balance that would be inferred from altimeter measurements of ice sheet elevations, using an assumed density of 917 kg/m^3. The ice sheet elevations are estimated using the model precipitation fields and the transfer function (2). (c) Difference between the results shown in Figure 2b and those shown in Figure 2a. These results represent the likely error in the altimeter secular mass estimates caused by not knowing the density through the top of the snow-ice column. The rms of the time series shown in Figure 2c is 4.5 mm/yr.

7000 years B.P.: so, 3000 years earlier than described in ICE-3G. We refer to this ice model as model B.

We also consider two possible addenda to the ICE-3G Antarctic ice model, which we denote as models C and D, each consisting of a uniform secular change in ice thickness during the last 4000 years with an amplitude of 30 mm/yr of water equivalent. This amplitude corresponds to about a 1.0-mm/yr change in global sea level and a total sea level change of ~4 m over the past 4000 years. For model C we assume that the ice mass has been decreasing at this rate (causing a rise in sea level), and for model D we assume the ice mass has been increasing (causing a fall in sea level). Note that models C and D include only the ice variability during the past 4000 years: that variability has not been added to ICE-3G. Because we are modeling PGR as a linear process, we can include the Earth's response to ice models C or D by simply adding it to the Earth's response to models A and B.

Our contention is that none of these proposed modifications to ICE-3G (i.e., either melting the ice earlier or additional melting/growth over the last 4000 years), or the various lower mantle viscosity values considered, are unambiguously refuted by existing data. By computing and comparing the rebound signals for these various models, we obtain some estimate of the uncertainty in the prediction of the effects of PGR on GLAS and GRACE.

Once we estimate the secular changes in the ice sheet elevation and in the geoid caused by one of these PGR models, we assume that the change is misinterpreted during GLAS and GRACE analyses as the effects of a secular variation in Antarctic ice mass. We estimate the secular ice mass variation that would be mistakenly inferred from the satellite data.

To do this for GLAS, we use the rebound models to compute the elevation change at each point of our 2.25°× 3.75° GLAS grid. For instance, if the rebound model predicts uplift of the crust, that will map directly into an apparent increase in the elevation of the ice surface. We average those gridded elevation changes over the ice sheet. We assume that the secular mass balance will be estimated by multiplying the elevation change by the density of ice (917 kg/m^3). Table 1 shows the estimated secular change in this inferred Antarctic mass averaged over the ice sheet, in millimeters of water equivalent, for the different rebound models. (To help understand the sign of the Table 1 results, note that model C, which involves a net loss of ice over the past 4000 years, leads to an inferred present-day increase in ice. This is because the PGR signal is the response of the solid Earth to this 4000-year deglaciation, and for model C that response involves crustal uplift.)

For GRACE we note that the secular change $\dot{T}(\theta, \phi)$ in the surface mass density at any point (θ, ϕ) will be inferred from the secular change in the geoid coefficients $\dot{C}_{lm}$ and $\dot{S}_{lm}$ using

$$\dot{T}(\theta,\phi) = \frac{a\rho_{\text{ave}}}{3}\sum_{l=0}^{\infty}\sum_{m=0}^{l}\tilde{P}_{lm}(\cos\theta)\frac{2l+1}{1+k_l} \times [\dot{C}_{lm}\cos(m\phi)+\dot{S}_{lm}\sin(m\phi)], \quad (4)$$

where ρ_{ave} is the average density of the Earth and the k_l are the elastic load Love numbers which describe the elastic deformation of the solid Earth caused by a change in ice mass [see *Wahr et al.*, 1998]. The secular change in ice thickness averaged over the entire ice sheet, expressed in units of water thickness, is

Table 1. Secular Change in Ice Mass Averaged Over Antarctica Inferred by GRACE and GLAS Analyses, Due to the Postglacial Rebound Signal Being Misinterpreted as a Mass Balance Signal

	GLAS, mm/yr				GRACE, mm/yr			
visc	A	B	C	D	A	B	C	D
4.5	5.8	3.7	2.7	-2.7	25.2	15.3	13.3	-13.3
10	5 3	3.7	1.9	-1.9	24.5	17.1	8.6	-8.6
50	2.5	2.0	1.0	-1.0	11.8	9.5	3.5	-3.5

The secular change in ice mass in mm/yr of water thickness. In all cases, the upper mantle viscosity is 10^{21} Pa s, and the lithospheric thickness is 120 km. "visc" refers to the lower mantle viscosity in units of 10^{21} Pa s. Ice models A-D are described in the text.

$$\dot{T}_{\text{ant}} = \frac{\int_{\text{ant}} \dot{T}(\theta,\phi)dA}{\rho_{\text{water}} A_{\text{ant}}}, \qquad (5)$$

where ρ_{water} is the density of water, the integral in (5) is over the Antarctic ice sheet, and A_{ant} is the area of the ice sheet.

We use the rebound models to estimate the secular change in the geoid coefficients (i.e., $\dot{C}_{lm}$ and $\dot{S}_{lm}$). We use those coefficients in (4) and use the resulting $\dot{T}$ in (5) to estimate the apparent secular change in Antarctic ice mass that would be erroneously inferred from the GRACE data. The results are shown in Table 1, for the various rebound models.

The Table 1 results show that the contamination of the ice mass estimates by the PGR signal is ~4-5 times more serious for GRACE than for GLAS. This is because the average density of the Earth's mantle is ~4-5 times the density of ice, so that the gravitational effect that accompanies 10 mm of crustal uplift is equivalent to the gravitational signal of 40-50 mm of ice.

In fact, the contamination of the GRACE results is large enough that it will probably be difficult to use GRACE data alone to substantially improve our knowledge of the present-day Antarctic mass balance. The Table 1 results suggest that the contamination of GRACE Antarctic mass balance results by the PGR signal could be anywhere from 38 mm/yr (for lower mantle viscosity equal to 4.5×10^{21} Pa s and Pleistocene ice model A and contemporary ice model C) to 2 mm/yr (for lower mantle viscosity equal to 4.5×10^{21} Pa s and ice models B and D). This suggests that the uncertainty in a GRACE-only mass balance estimate due to the PGR signal might be on the order of ± 20 mm/yr of water, corresponding to about ± 0.6 mm/yr of sea level change. This result is consistent with the conclusions of *Bentley and Wahr* [1998]. (Note, incidentally, that this ±0.6-mm/yr uncertainty is still better than a factor of 2 improvement over the estimated present-day uncertainty of ± 1.4 mm/yr described by *Houghton et al.* [1996].)

For GLAS the PGR signals shown in Table 1 could cause an apparent Antarctic mass balance estimate of anywhere from 1.0 mm/yr (viscosity equal to 4.5×10^{21} Pa s; ice models B and D) to 8.5 mm/yr (viscosity equal to 4.5×10^{21} Pa s; ice models A and C). Expanding this range of values slightly, we tentatively estimate the contamination of the GLAS mass balance estimate by the PGR signal as somewhere between 0 and 10 mm/yr equivalent water thickness (corresponding to between 0 and about −0.3 mm/yr of global sea level rise). This suggests that we attach an uncertainty to the GLAS mass balance estimates of about ±5 mm/yr (water equivalent), due to possible errors in the PGR model. This is the same level of error as that caused by compaction (see section 3.2).

5. Combining GLAS and GRACE Measurements

Here we describe a method of using GRACE data to reduce the PGR contributions to the GLAS measurement errors. In effect, GLAS is sensitive to one linear combination of PGR and present-day ice balance, and GRACE is sensitive to another. So by using both measurement types we can determine two linear combinations of these two variables and so can estimate each variable separately. As we shall see, the effectiveness of this approach depends on the compaction error.

Our proposed method of combining the two data types is iterative. We assume 5 years of coincident measurements for each satellite. We initially use the GLAS data alone to determine the secular rate of change in ice mass averaged over Antarctica. We refer to this initial estimate as the zeroth iteration. We could make this initial estimate either after removing an independently determined PGR model from the original GLAS data or without making any attempt to model the PGR effects. For the simulated results described in section 5.2 we have not used any PGR model to reduce the GLAS data for the zeroth iteration. In either case, the

mass balance estimates would almost certainly be contaminated by PGR effects, since PGR models contain errors.

To iterate, we compute the secular rate of change in the geoid caused by this zeroth order GLAS mass balance estimate and remove that geoid signal from the GRACE data. The secular geoid change inferred from the residual GRACE data is then interpreted as being due entirely to PGR. This estimate of the PGR geoid signal is used to compute the PGR crustal uplift signal, using a method described in section 5.1 below. This crustal uplift PGR estimate is removed from GLAS, and the residuals are used to determine a better ice balance estimate. We refer to this estimate as the first iteration.

We repeat the process: compute the geoid contributions from this new GLAS ice mass estimate and remove them from GRACE, interpret the secular component of the new GRACE residuals as the effect of PGR and remove it from GLAS, and use the GLAS residuals to construct a further improved ice balance estimate, which is referred to as the second iteration. We can continue iterating in this manner indefinitely.

5.1. Estimating PGR Uplift From the PGR Geoid Change

During this iterative process we must estimate the PGR crustal uplift rates (to remove from GLAS) from knowledge of the PGR secular geoid changes (inferred from GRACE). We have discovered a method of doing this that does not require assumptions about the ice model or viscosity profile.

Let

$$\dot{N}^{\mathrm{PGR}}(\theta,\phi) = a\sum_{l=0}^{\infty}\sum_{m=0}^{l}\tilde{P}_{lm}(\cos\theta)\,[\dot{C}_{lm}^{\mathrm{PGR}}\cos(m\phi) + \dot{S}_{lm}^{\mathrm{PGR}}\sin(m\phi)] \quad (6)$$

be the contribution of PGR to the secular rate of change in the geoid, where $\dot{C}_{lm}^{\mathrm{PGR}}$ and $\dot{S}_{lm}^{\mathrm{PGR}}$ represent the rates of change of the geoid coefficients (see equation (1)). Similarly, let

$$\dot{U}^{\mathrm{PGR}}(\theta,\phi) = a\sum_{l=0}^{\infty}\sum_{m=0}^{l}\tilde{P}_{lm}(\cos\theta)[\dot{A}_{lm}^{\mathrm{PGR}}\cos(m\phi) + \dot{B}_{lm}^{\mathrm{PGR}}\sin(m\phi)] \quad (7)$$

be the uplift rate of the Earth's surface caused by PGR, where $\dot{A}_{lm}^{\mathrm{PGR}}$ and $\dot{B}_{lm}^{\mathrm{PGR}}$ are the Legendre expansion coefficients of $\dot{U}^{\mathrm{PGR}}$. We have found that to a high degree of approximation,

$$\dot{A}_{lm}^{\mathrm{PGR}} = \left(\frac{2l+1}{2}\right)\dot{C}_{lm}^{\mathrm{PGR}}, \quad (8)$$

$$\dot{B}_{lm}^{\mathrm{PGR}} = \left(\frac{2l+1}{2}\right)\dot{S}_{lm}^{\mathrm{PGR}} \quad (9)$$

We were led to this approximation because of the results of *Wahr et. al.* [1995, equation (8)], who discovered a similar relation between surface gravity and uplift. The explanation for (8) and (9) is that the secular change in the geoid caused by PGR is mostly due to mass anomalies associated with vertical motion of the surface (see *Wahr et. al.* [1995]). This approximation works well for every viscosity profile and ice model we have considered (though we have not considered rheological models with low-viscosity channels). As an example, Figure 3a shows the crustal uplift rate $\dot{U}^{\mathrm{PGR}}$ as computed from a PGR model that uses the elastic structure from PREM [*Dziewonski and Anderson*, 1981], with lower mantle viscosity 10^{22} Pa s, upper mantle viscosity 10^{21} Pa s, and lithospheric thickness 120 km, and that convolves with the ICE-3G Pleistocene ice model of *Tushingham and Peltier* [1991]. Figure 3b shows the approximate uplift, computed by finding the PGR geoid coefficients $\dot{C}_{lm}^{\mathrm{PGR}}$ and $\dot{S}_{lm}^{\mathrm{PGR}}$ for the same viscosity profile and ice model and then using (8), (9), and (7) to find the uplift rates. Note the similarity between Figures 3a and 3b. Figure 3c shows the difference, which is almost negligible on the scale used in Figure 3.

5.2. A Simulation

We use 5 years of simulated monthly GLAS and GRACE data, constructed as described in section 2. We apply the iteration process described above to estimate the 5-year secular change in mass averaged over Antarctica. We do this first without including contributions from a varying accumulation rate in our simulated data. Thus there is no compaction error in this initial case. Figure 4a shows the results for the estimated ice thickness change (in mm/yr of water thickness equivalent), as a function of iteration number. For this simulation we compute the PGR contribution using an ice model that is the sum of ICE-3G and an assumed thinning of 30 mm/yr averaged over the last 4000 years. The viscosity profile is the same as that used for Figure 3. The present-day thinning of the ice sheet due to horizontal flow was chosen to be 30 mm/yr of water equivalent thickness, coincident with the assumed thinning rate over the last 4000 years. Since no variable accumulation has been added, the "correct" value of the average Antarctic ice thickness change for this 5-year period is -30 mm/yr (solid line in Figure 4a). (Note that the absence of variable accumulation implies that the century-scale trend would also equal -30 mm/yr.)

The result of the zeroth iteration (i.e., GLAS alone; no GRACE data) is about -23 mm/yr. This error is almost entirely due to contamination from PGR. The contribution from GLAS measurement errors is found to be on the order of -0.05 mm/yr, consistent with the discussion in section 2.3. When GRACE data are in-

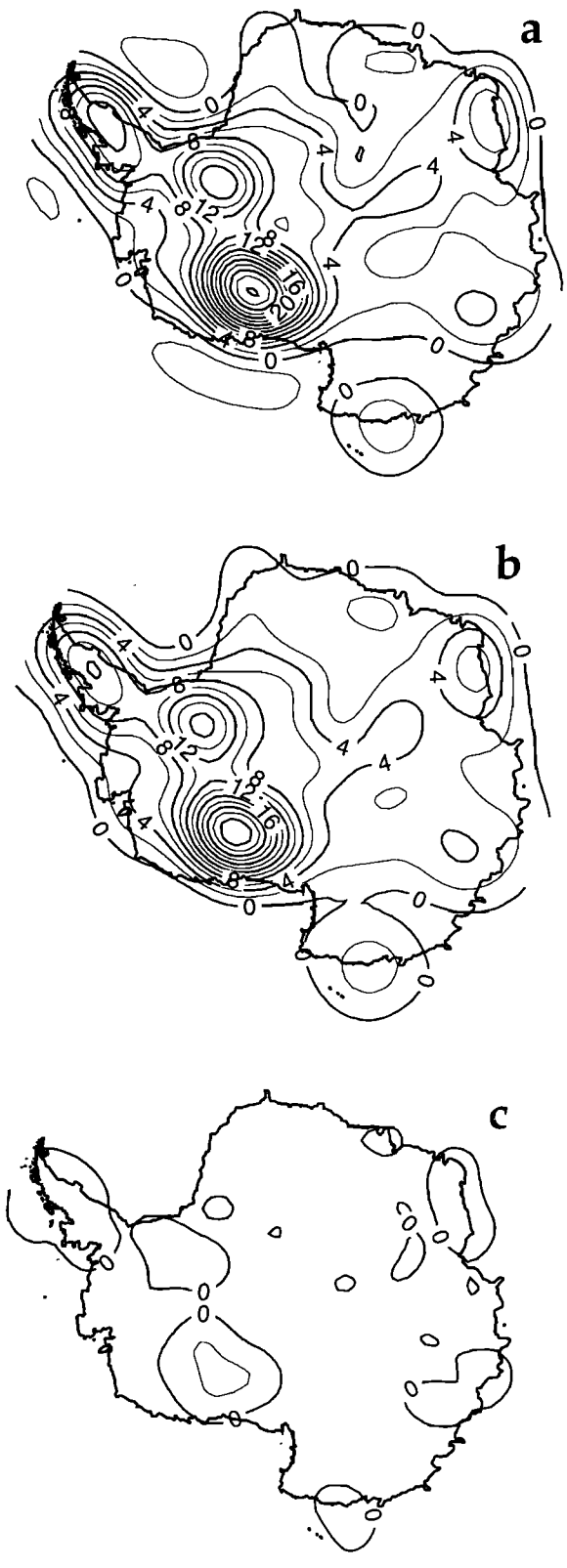

Figure 3. (a) Crustal uplift computed by the PGR model described in the text. (b) Crustal uplift generated by using the model to compute the secular change in the geoid and then inferring the uplift using the approximations (8) and (9). (c) Difference between Figures 3a and 3b. The units in these plots are mm/yr, and the contour interval is 2 mm/yr.

cluded and the iteration number increases, the inferred ice thickness estimate converges closely (a difference of +0.05 mm/yr) to the correct -30-mm/yr value: The use of GRACE data has effectively removed the PGR error in the GLAS estimate. The remaining small difference from the correct value is due to a combination of satellite errors (both GLAS and GRACE), to contamination of the GRACE data by secular atmospheric pressure errors and oceanic and hydrological mass fluctuations, and to whatever inadequacies exist in the approximations (8) and (9).

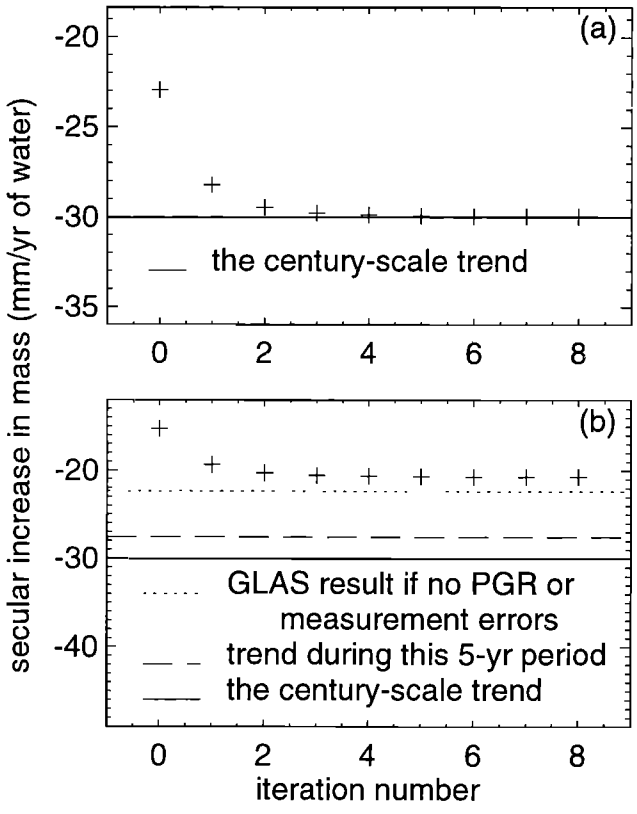

Figure 4. Secular change in mass inferred from 5 years of simulated monthly GLAS and GRACE data. The zeroth iteration does not use GRACE data. The solid line is the century-scale trend used in the simulation. (a) This simulation did not include the effects of Antarctic precipitation either on GLAS (ice sheet elevations) or on GRACE (geoid contributions). After several iterations the mass balance result converges to the correct value. Thus combining with GRACE data has removed the PGR error. (b) This simulation includes the effects of Antarctic precipitation for one 5-year period of the CSM-1 output. The long-dashed line is the mass balance rate during this 5-year period. The difference between the long-dashed and solid lines is the undersampling error. The short-dashed line is the secular mass change that would be inferred from GLAS for this 5-year period, if there were no PGR contribution or GLAS measurement errors. It differs from the mass balance rate over this 5-year period because of the compaction error. After several iterations with GRACE the mass balance result differs from the 5-year rate by ~1.3 times the compaction error.

Next we go through this procedure again, after adding the variable accumulation contributions to the GLAS and GRACE data through the effects of the accumulation on ice sheet elevations (for GLAS) and on the geoid (for GRACE). This introduces a compaction error into the GLAS estimate of the 5-year trend in mass. It also causes the 5-year trend to differ from the multicentury trend; that is, it introduces an undersampling error. The amplitudes of these errors depend on which 5-year period of accumulation data is chosen, and so we go through this simulated solution for every nonoverlapping 5-year interval in the 2048-month data set of climate model output and inferred ice sheet elevations. Figure 4b shows the results for the estimated ice thickness change as a function of iteration number for one such 5-year period. The PGR model is the same as for Figure 4a. As usual, the century-scale trend in mass used for this simulation is -30 mm/yr, water equivalent (solid line). When the variable accumulation is added to the assumed present-day 30-mm/yr horizontal thinning rate, the mass change for this particular 5-year period becomes about -27.6 mm/yr, water equivalent (long-dashed line). Thus the difference between the solid and long-dashed lines (i.e., 2.4 mm/yr) is the undersampling error in determining the century-scale trend. The GLAS compaction error for this 5-year period is ~5.2 mm/yr. So if there were no GLAS measurement errors and no PGR contribution, the inferred thickness change from GLAS alone would be about -22.4 mm/yr (short-dashed line). When the PGR contribution is included, the estimate from the zeroth iteration is -15.3 mm/yr. Thus the total error in estimating the century-scale trend in mass (in water equivalent thickness) is ~14.7 mm/yr. The total error in estimating the 5-year surface mass balance rate is 12.3 mm/yr. The difference shown in Figure 4b between the result for the zeroth iteration and the short-dashed line is almost entirely due to the PGR contamination of the GLAS results: The effects of the GLAS measurement errors are on the order of only 0.05 mm/yr.

When the GRACE data are included and the iteration number increases, the ice thickness estimate improves but does not converge to the short-dashed line. Evidently, the use of the GRACE data does not entirely remove the PGR error in the GLAS result. We will refer to the difference between the short-dashed line and the ice thickness value for large iteration number as the final PGR error, although it also includes small contributions from GRACE and GLAS measurement errors and from contamination of the GRACE data from atmospheric and oceanic and hydrological gravity signals. This final PGR error works out to be ~1.6 mm/yr, which is roughly 0.3 of the 5.2-mm/yr compaction error.

The final PGR error is not closer to zero because every time during the iteration process that we use the GLAS mass balance estimates to compute the geoid and remove it from the GRACE data, we are introducing the effects of the GLAS compaction error into the GRACE results. Thus the PGR estimates from these GRACE residuals are degraded by that compaction error.

Figure 5 summarizes the simulation results for all 5-year simulation periods. Shown are the final PGR error (i.e., the difference between the thickness change for large iteration number and the thickness change that would be estimated from GLAS alone in the absence of a PGR signal and GLAS measurement errors) as a function of the compaction error for that 5-year period. The points lie almost exactly on a straight line, with a best fitting slope of 0.31. We conclude that the final PGR error, after using both GLAS and GRACE data in our iterative procedure, is likely to be 0.31 times the compaction error. Thus the total error in the estimated 5-year surface mass balance rate from all sources is 1.31 times the compaction error. If the typical compaction error is ±4.5 mm/yr, as suggested in section 3.2, then the final error in the GLAS plus GRACE 5-year rate estimate is on the order of ±6 mm/yr, equivalent to an error in the Antarctic contribution to global sea level rise of about ±0.2 mm/yr. Since the undersampling error has an rms of ~3 mm/yr and is in phase with the compaction error (see section 3), we can add this 3-mm/yr undersampling error to the 6-mm/yr error in the 5-year rate estimate, to conclude that GLAS plus GRACE should be able to determine the multicentury trend to an rms accuracy of about ±9 mm/yr, equivalent to a contribution of about ±0.3 mm/yr to global sea level rise.

6. Discussion

We have discussed the use of GLAS and GRACE measurements to estimate the secular trend in the to-

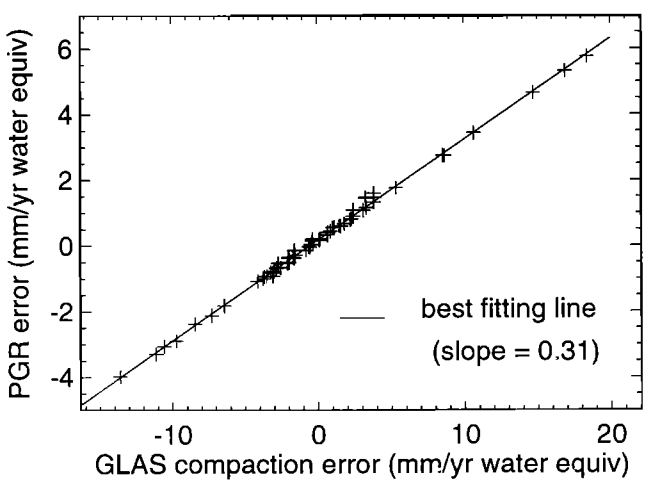

Figure 5. Final PGR error remaining after many iterations of GLAS and GRACE, as a function of the compaction error, for every nonoverlapping 5-year period in the 219-year data set. The best fitting line is superimposed on the data and has a slope of 0.31.

tal mass of the Antarctic ice sheet. To study the mass imbalance from glaciological and climatic perspectives, the most fundamental quantity is the secular trend over timescales of a century or longer, since the variability of large-scale ice flow tends to occur on those sorts of timescales. Perhaps there will eventually be data from enough consecutive satellite missions to be able to address century-scale variability directly. In the meantime, a more modest but more easily attainable objective is the mass balance rate over the lifetime of a single, or perhaps a few, successive missions. Using the results in this paper, we can estimate the errors in determining both these quantities, i.e., both the century-scale trend and the mass balance rate over one or more mission lifetimes.

There will be two significant sources of error when using GLAS altimeter data alone to infer the secular change in the total mass of the Antarctic ice sheet. One is the uncertainty in the PGR model used to predict Antarctic crustal uplift. The other is the fact that the accumulation rate will be variable at periods significantly shorter than a century. For this application the GLAS measurement errors are substantially less important than either of these error sources. The measurement errors would be relatively more important when estimating the mass balance of subregions within the Antarctic ice sheet.

The effects of a variable accumulation rate can be further separated into what we have termed undersampling and compaction errors. The undersampling error refers to the fact that because ICESat will have, at most, a 5-year lifetime, it will not be possible to separate decadal and interannual variability from the longer-term secular trend. If the objective is only to determine the linear trend over the 5-year lifetime, then this would not be an error at all. If, on the other hand, the goal is to determine the century-scale trend, then the results described in section 3.1 suggest that because of the natural decadal and interannual variability in accumulation pattern the 5-year secular trend in total Antarctic mass is apt to differ from the century-scale trend by, on average, about ±3 mm/yr equivalent water thickness, corresponding to an Antarctic contribution to global sea level change of about ±0.1 mm/yr. By taking longer-term averages of the accumulation data we have found that this error decreases roughly as the inverse square root of the mission lifetime. For example, suppose that there were enough consecutive altimeter missions to provide 15 years of continuous measurements. In that case, the undersampling error would reduce to about $\pm 3/\sqrt{3} \approx \pm 1.7$ mm/yr of equivalent water thickness.

The compaction error is caused by inadequate knowledge of the density profile in the upper layers of the snow-ice column, which is needed to infer the change in mass from the altimeter measurements of changes in ice sheet elevations. The compaction error causes an error in the GLAS estimate of the 5-year mass trend (and hence also of the multicentury trend). It is in phase with the undersampling error, and ~1.5 times as large, with an rms amplitude of the order of ±4.5 mm/yr equivalent water thickness after 5 years (section 3.2). Thus the total error caused by the variable accumulation in determining the century-scale mass trend is the sum of the undersampling and compaction errors and so is on the order of ±7.5 mm/yr.

The GR error is discussed in section 4. Like the compaction error, the PGR error degrades the GLAS estimate of the 5-year mass trend. The PGR error is hard to quantify but is likely to be about ±5-mm/yr in equivalent water thickness. Thus the effects of the PGR and compaction errors are approximately equal.

It is not clear how best to combine the undersampling, compaction, and PGR errors into a single uncertainty, since the probability distribution of the PGR error is difficult to estimate. For this discussion we will assume no correlation between the PGR errors and the other errors and will interpret the ±5-mm/yr PGR error as a 1-sigma Gaussian error. In this case, the 1-sigma uncertainty in total thickness will be the square root of the sum of the PGR variance (25 $(\text{mm/yr})^2$) and the other variances.

The second and third columns of Table 2 show 1-sigma error estimates for using altimeter data alone to infer both the century-scale trend and the error in the mass balance rate over the entire altimeter data span. Results are given assuming a single mission length (5 years) and assuming multiple, successive missions, for up to 20 years of continuous data. The results should be divided by ~30 to obtain the uncertainty in the Antarctic contribution to global sea level rise. The Table 2 results should be viewed with caution, since they are dependent on the unverified model precipitation fields and on an incomplete assessment of the PGR error. There is, especially, no justification for providing the results to two significant figures. That is done in Table 2 only to better illustrate what happens when the cumulative mission length increases and when the gravity data are added.

The Table 2 results for the altimeter alone show that the results do not improve much with increasing mission length, particularly when determining the trend over just the mission lifetime. This is due to the PGR error, which is fundamentally different from the compaction and undersampling errors. Those latter errors tend to decrease with the square root of the mission length. However, a longer mission does nothing to improve the PGR error. That error is better viewed as a bias, which remains constant as the data span increases. So for long mission lifetimes the total uncertainty converges to the assumed ±5-mm/yr PGR error.

Adding time-variable gravity from a satellite mission such as GRACE can overcome this problem. Satellite gravity, alone, cannot deliver the secular change in ice thickness nearly as well as can an altimeter. There is no compaction error for the gravity measurements, but the effects of PGR on geoid fluctuations are 4-5 times larger

Table 2. Estimated Error in the Secular Change in Antarctic Ice Mass That Could Be Inferred by Altimeter Data Alone and by a Combination of Altimeter and Gravity Data

	Altimeter Only		Altimeter Plus Gravity	
Cumulative Mission Length, years	Error in Century-Scale Trend, mm/yr water equiv	Error in Trend Over Data Span, mm/yr water equiv	Error in Century-Scale Trend, mm/yr water equiv	Error in Trend Over Data Span, mm/yr water equiv
5	9.0	6.7	8.9	5.9
10	7.3	5.9	6.3	4.2
15	6 6	5.6	5 1	3.4
20	6.2	5.5	4 4	2.9

Results are shown for multiple, successive missions, for up to 20 years of continuous data The estimated errors are given in mm/yr of water thickness. Here, "equiv," equivalent.

than they are on vertical crustal motion. However, by combining altimeter and gravity data taken at the same time, the PGR error in the altimeter measurements can be reduced to ~30% of the compaction error. This remaining PGR error has the same sign as the compaction error, so that the two errors add constructively.

The fourth and fifth columns of Table 2 show the estimated uncertainties when the altimeter and gravity data are combined. Note that for a 5-year mission there is only marginal improvement when adding the gravity data, particularly when estimating the secular-scale trend. On the other hand, it should be emphasized that the uncertainty in the PGR models is poorly known. Our assumed ±5-mm/yr uncertainty in the GLAS estimates caused by PGR errors is inferred from an incomplete suite of possible ice models and viscosity profiles. It is not inconceivable that the altimeter-only uncertainties shown in Table 2 underestimate the true uncertainty. By including the gravity data in the solution the PGR error is reduced to 30% of the compaction error, no matter how accurate the PGR model is. Thus the altimeter plus gravity results in Table 2 are independent of the accuracy of the PGR model.

The advantage of combining with gravity becomes most evident for longer cumulative mission lengths. After 10 years or so, altimetry without gravity comes up against a fundamental limit in accuracy caused by the uncertainty in the PGR uplift. Once this limit is reached, continued altimetric observations alone cannot provide much further improvement. By introducing satellite gravity measurements into the solution process this limit is overcome, and the total mass balance uncertainty converges toward zero with increasing observing period.

7. Two Caveats

Our conclusions are dependent on the assumption that the CSM-1 climate model adequately reproduces the general spatial and temporal characteristics of Antarctic accumulation. This is a difficult assumption to assess, as discussed in section 2.1, and we are not able to quantify its level of uncertainty.

In general terms, if CSM-1 significantly underestimates the temporal variability in Antarctic accumulation, then the compaction error could conceivably become notably larger than the PGR error. After combining GLAS and GRACE data the total remaining error in determining the 5-year mass balance rate is ~1.3 times the compaction error alone. So if the compaction error were significantly larger than that inferred in section 2.1, this final error could well be larger than the sum of the compaction error and the original PGR error that affected the GLAS-only analysis before the addition of GRACE. Conversely, if CSM-1 significantly overestimates the temporal variability, then the compaction error would be smaller than that inferred here, and the advantage of combining with GRACE data would become more pronounced.

Our other caveat is that our method of combining GRACE and GLAS data makes use of the approximate relations (8) and (9) to transform the geoid change inferred from GRACE to the crustal uplift signal that affects GLAS. We have found that approximation to work well if the Earth's viscosity profile is spherically symmetric. Mineralogical arguments suggest that there could be large, thermally driven, lateral variations in viscosity, particularly in the upper mantle. Incorporating aspherical viscosity into a PGR model is a difficult problem that is just now beginning to receive attention. We do not presently know how large the effects of lateral viscosity are, nor do we know whether those effects, large or small, would have a significant impact on the approximations (8) and (9).

Acknowledgments. We thank Dazhong Han for providing his elastic Love numbers and viscoelastic Green's functions; Gordan Bonan for the CSM-1 precipitation data, Mike Watkins, Brooks Thomas, and Srinivas Bettadpur for their estimates of the GRACE gravity field errors; Mery Molenaar and Frank Bryan for their estimates of the geoid

coefficients due to the ocean, Chris Milly and Krista Dunne for their global, gridded water storage data set, Bob Schutz and C. K. Shum for discussion of the GLAS measurement errors, and David Bromwich, Erik Ivins, and Jay Zwally for comments on the manuscript. This work was partially supported by NASA grant NAG5-7703 and NSF grant EAR-9526905 to the University of Colorado, by U. K. Natural Environmental Research Council grants GR3/11186 and F14/6/39, and by NASA contract NAS5-33015 to the University of Wisconsin - Madison.

References

Arthern, R.J., and D.J. Wingham, The natural fluctuations of firn densification and their effect on the geodetic determination of ice sheet mass balance, *Clim. Change, 40,* 605-624, 1998.

Bentley, C.R., and J.M. Wahr, Satellite gravity and the mass balance of the Antarctic ice sheet, *J. Glaciol., 44,* 207-213, 1998.

Boville, B. A., and P. Gent, The NCAR climate system model, version one, *J. Clim., 11,* 1115-1130, 1998.

Briegleb, B.P., and D.H. Bromwich, Polar climate simulation of the NCAR CCM3, *J. Clim., 11,* 1270-1281, 1998.

Choe, C., Estimation of ice sheet surface elevation change from the Geoscience Laser Altimeter satellite crossover simulation, Univ. of Tex. at Austin, Cent. for Space Res., 1997.

Dickey, J.O., et al., *Satellite Gravity and the Geosphere: Contributions to the Study of the Solid Earth and Its Fluid Envelope*, 112 pp., Natl. Acad Press, Washington, D C., 1997

Dukowicz, J K , and R D Smith, Implicit free-surface method for the Bryan-Cox-Semtner ocean model, *J. Geophys. Res., 99,* 7991-8014, 1994

Dziewonski, A., and D.L. Anderson, Preliminary reference Earth model, *Phys. Earth Planet. Inter., 25,* 297-356, 1981.

Giovinetto, M.B., D.H. Bromwich, and G Wendler, Atmospheric net transport of water vapor and latent heat across 70°S, *J. Geophys. Res., 97,* 917-930, 1992.

Han, D and J. Wahr, The viscoelastic relaxation of a realistically stratified Earth, and a further analysis of postglacial rebound, *Geophys. J. Int., 120,* 287-311, 1995.

Houghton, J.T., L.G. Meira Filho, B A. Callander, N. Harris, A. Kattenberg, and K. Maskell, (Eds.), Climate Change 1995: The Science of Climate Change, 572 pp., Cambridge Univ. Press, New York, 1996.

James, T.S., and E. R. Ivins, Predictions of Antarctic crustal motion driven by present-day ice sheet evolution and by isostatic memory of the Last Glacial Maximum, *J. Geophys. Res., 103,* 4993-5017, 1998.

Mitrovica, J.X., J.L Davis, and I.I. Shapiro, A spectral formalism for computing three-dimensional deformations due to surface loads, 1, Theory, *J. Geophys. Res., 99,* 7057-7073, 1994.

Oerlemans, J., Effect of irregular fluctuations in Antarctic precipitation on global sea level, *Nature, 290,* 770-772, 1981.

Press, W.H., S.A. Teukolsky, W.T. Vetterling, and B.P. Flannery, *Numerical Recipes: The Art of Scientific Computing*, 2nd ed., 963 pp. Cambridge Univ. Press, New York, 1992.

Tushingham, A.M., and W.R. Peltier, ICE-3G: A new global model of late Pleistocene deglaciation based upon geophysical predictions of postglacial relative sea level change *J. Geophys. Res., 96,* 4497-4523, 1991.

Van der Veen, C.J., Interpretation of short-term ice-sheet elevation changes inferred from satellite altimetry, *Clim. Change, 23,* 383-405, 1993.

Wahr, J.M., D. Han, and A. Trupin, Predictions of vertical uplift caused by changing polar ice volumes on a viscoelastic Earth, *Geophys. Res. Lett., 22,* 977-980, 1995.

Wahr, J., M. Molenaar, and F. Bryan, Time-variability of the Earth's gravity field: hydrological and oceanic effects and their possible detection using GRACE, *J. Geophys. Res., 103,* 30,205-30,230, 1998.

Wingham, D.J., Short fluctuations in the mass, density and thickness of a dry firn column, *J. Glaciol.,* in press, 2000.

Wingham, D.J., A.R. Ridout, and C K. Shum, Antarctic elevation change 1992 to 1996, *Science, 282,* 456-458, 1998.

C. Bentley, Department of Geology and Geophysics, University of Wisconsin, 1215 West Dayton Street, Madison, WI 53706. (bentley@geology.wisc.edu)

J. Wahr, Department of Physics and Cooperative Institute for Research in Environmental Sciences, University of Colorado at Boulder, Campus Box 390, Boulder, CO 80309-0390. (wahr@lemond.colorado.edu)

D. Wingham, Department of Space and Climate Physics, University College London, London, WC1H OAH, England, U.K.

(Received July 29, 1999; revised March 3, 2000;
accepted April 3, 2000.)